Chemical Science

EDGE ARTICLE

Check for updates

Super electron donors derived from diboron†

Li Zhang and Lei Jiao ⬤ *

Single-electron transfer is an important process in organic chemistry, in which a single-electron reductant (electron donor) acts as a key component. Compared with metal-based electron donors, organic electron donors have some unique advantages, such as tunable reduction ability and mild reaction conditions. The development of novel organic electron donors with good reduction ability together with ease of preparation is in high demand. Based on the pyridine-catalyzed radical borylation reaction developed in our laboratory, we have discovered that, the reaction system consisting of a diboron(4) compound, methoxide and a pyridine derivative could smoothly produce super electron donors *in situ*. Two boryl–pyridine based species, the major one being a *trans*-2*H*,2′*H*-[2,2′-bipyridine]-1,1′-diide borate complex and the minor one being a pyridine radical anion–borate complex, were observed and carefully characterized. These complexes were found to be organic super electron donors unprecedented in literature, and their formation mechanisms were studied by DFT calculations. The diboron/methoxide/pyridine system enables the preparation of organic super electron donors from easily accessible starting materials under mild conditions, which has the potential to be a general and practical single-electron reducing agent in organic synthesis.

Introduction

Single-electron transfer (SET) is an important process in various redox- and radical-type organic reactions,[1] where a single-electron reductant (electron donor) plays an important role. Usually, single-electron reductants involved in these reactions include alkali metals, alkali earth metals, low valent metallic reagents (*e.g.*, SmI$_2$ and TiCl$_3$) and organometallic reagents (*e.g.*, sodium naphthalide, Cp$_2$Ti^{III}),[2] which have been used in organic chemistry for more than half a century. Compared with these traditional electron donors, organic electron donors have attracted the attention of organic chemists more recently due to their tunable reducing ability and mild reduction conditions.

Tetrathiafulvalene (TTF) and tetrakis(dimethylamino)-ethylene (TDAE) have long been known as organic electron donors, but they exhibit moderate reducing ability and can only be used in the reduction of a limited number of substrates.[3] Since 1993, Murphy and co-workers have developed a series of organic electron donors based on electron-rich alkenes (*e.g.*, **1**), which exhibit potent reduction abilities (Scheme 1a).[4] The sufficiently low oxidation potential even allows them to promote single-electron reduction of aryl iodides, and thus they are regarded as "super electron donors" (SEDs).[4,5] These

structurally well-defined SEDs can efficiently promote a series of single-electron reductions and radical-type reactions;[4] however, the structural complexity and the requirement for multi-step synthesis limit their utility in synthesis to some extent. Due to the importance of single-electron reducing agents in organic chemistry, the development of novel organic electron donors with good reduction ability, tunable structure, and a simple preparation procedure compared to traditional metal-based electron donors will significantly advance organic redox chemistry.
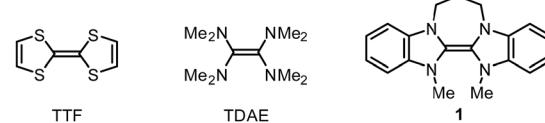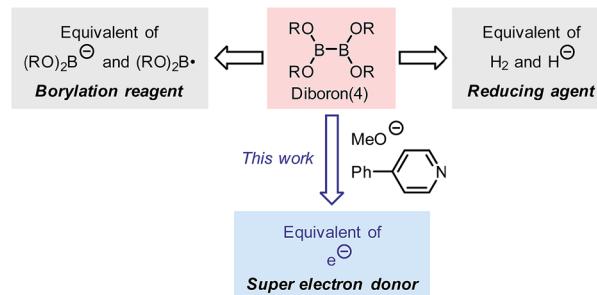
Center of Basic Molecular Science (CBMS), Department of Chemistry, Tsinghua University, Beijing 10084, China. E-mail: Leijiao@mail.tsinghua.edu.cn

† Electronic supplementary information (ESI) available: Experimental procedures, characterization data, simulation of the EPR spectrum and computational details. CCDC 1578447 and 1585926. For ESI and crystallographic data in CIF or other electronic format see DOI: 10.1039/c8sc00008e

Scheme 1 Organic electron donors.

Recently, we reported a pyridine-catalyzed radical borylation reaction of aryl halides employing diboron(4) compounds as the boron source.[6] The preliminary mechanistic study revealed that diboron, methoxide and the pyridine catalyst formed a reductive mixture, which promoted single-electron reduction of the aryl halide to produce an aryl radical as the key intermediate. The electron donor formed in the reaction system exhibited comparable reduction ability to previously reported SEDs and is rather attractive due to the ease of preparation. However, the structure of the electron donor was not clearly elucidated in the previous study, nor was its synthetic potential extensively exploited.

Although diborons have been employed as reducing agents in several reduction reactions as either hydrogen or hydride equivalents,[7] to the best of our knowledge, there is no precedent to the use of diboron as the precursor to a structurally well-defined single-electron reductant. Thus, the investigation into the SEDs derived from diborons is significant. In this work, we demonstrate that the combination of diboron, pyridine and a base can be used as an efficient source of structurally well-defined SEDs (Scheme 1b). The structures of the electron donors in the reaction system have been clearly elucidated, leading to the discovery of two novel boron–pyridine based SEDs. The detailed mechanism of their formation and inter-conversion has also been disclosed, which represents a novel activation mode of the boron–boron bond in diboron(4) compounds. This reaction system is able to promote single-electron reduction of a variety of substrates and able to trigger radical chain reactions initiated by SET. Due to this feature, the SEDs derived from diboron have the potential to be used as a general and practical single-electron reducing agent in organic synthesis. Herein we report the details of our investigation on SEDs derived from diborons via a combined experimental and DFT computational study.

Results and discussion

Since the reaction between diboron, methoxide and a pyridine derivative was found to exhibit electron-donating ability in the radical borylation reaction, we sought to make clear the following points:

(1) The structure of the electron donor produced in the diboron/methoxide/pyridine system;

(2) The formation mechanism of the electron donor;

(3) The potential application of the reduction system to other electron-transfer-related reactions.

Because 4-phenylpyridine (2) showed the best performance in the borylation reaction of aryl halides, we chose the reaction system consisting of bis(pinacolato)diborane, methoxide and pyridine derivative 2 as a model throughout our study.

1. Elucidation of electron donor structure

It was found in our previous study that by simply mixing B_2pin_2, MeOK and 2 in DMSO, a deep purple color emerged and an intense EPR signal was detected, which was attributed to the formation of the electron donor in this reductive mixture.[6]
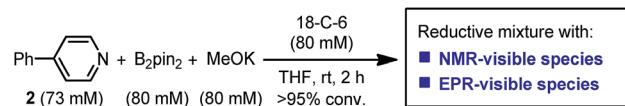
Scheme 2 Reaction conditions of the model study.

However, the poor solubility of methoxide in DMSO led to a limited concentration of the electron donor, which hampered further structural characterization. To prepare a solution of the SED with a reasonable concentration, we used 18-crown-6 (18-C-6) as an additive and performed the reaction in THF. To our delight, the mixture of B_2pin_2, MeOK, 18-C-6 and 2 in THF formed a homogenous deep purple solution. Quite unexpectedly, the solution exhibited well-resolved signals in both NMR and EPR spectra (Scheme 2). This observation was in contrast with the previous proposal, where only two radical species were generated in this reaction mixture. Therefore, we set out to carefully characterize the observed species.

Structure of the NMR-visible species. The ^{1}H-NMR spectrum of the aforementioned reaction mixture was quite clear, and the aromatic region showed that pyridine 2 was cleanly transformed to a major species with ca. 77% yield (Fig. 1). The peaks corresponding to the phenyl group showed only minor changes in chemical shift, while the peaks of the pyridine ring (two doublets, 2H each) changed dramatically (upfield-shifted to four separate peaks, 1H each). The change in the spectral pattern, together with the result from the 1D NOESY experiment, implied the formation of a dearomatized pyridine ring, where two chemical bonds were connected to the 1- and 2-positions (Fig. 1b). ^{11}B-NMR (formation of a new singlet at 6.2 ppm) was indicative of a tetracoordinated boron center. ^{13}C-NMR and HSQC spectra showed that boron was not directly attached to carbon since no quadrupolar broadening was observed in ^{13}C-NMR spectroscopy. Although NMR analysis provided important clues for structural assignment, more information is required to determine the precise structure of this species.

We sought to characterize the structure of this species by single-crystal X-ray diffraction (XRD) analysis, but it was
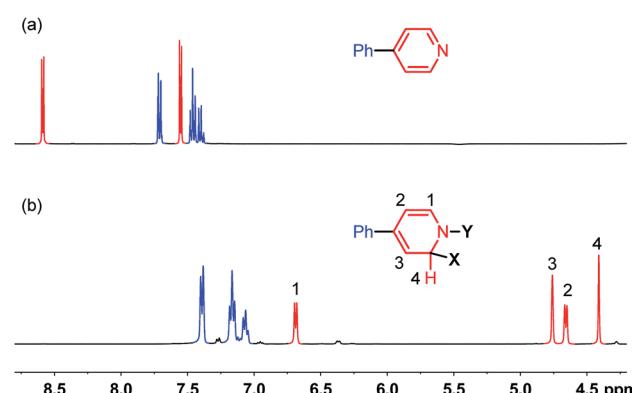

Fig. 1 ^{1}H-NMR spectra (400 MHz) of (a) 4-phenylpyridine and (b) reaction mixture shown in Scheme 2 at room temperature in THF.
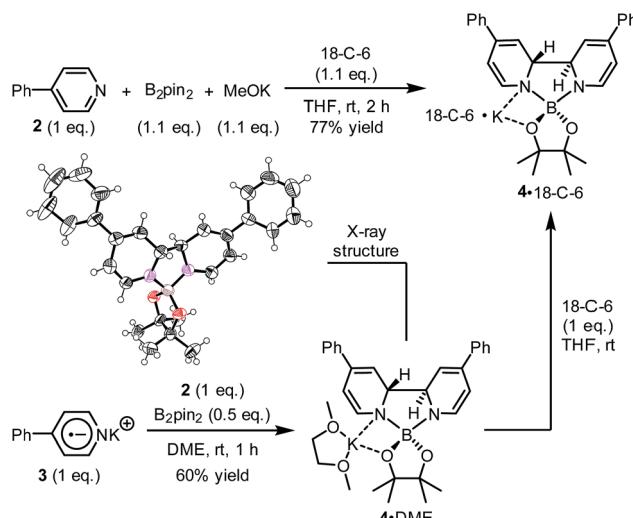
Scheme 3 Independent preparation of the NMR-visible species. In the X-ray structure of compound **4**, the DME part and the potassium cation are omitted for clarity. Thermal ellipsoids are drawn at 50% probability level.

difficult to directly crystallize it from the reaction mixture. Fortunately, we discovered that the reaction of 4-phenylpyridine radical anion (**3**) with B$_2$pin$_2$ in the presence of excess **2** in DME could afford a pale yellow crystalline solid upon the addition of hexane. After treatment with 18-C-6 in THF, it produced identical ^{1}H-, ^{13}C- and ^{11}B-NMR spectra as the previously acquired ones of the reaction mixture, confirming the same identity of the NMR-visible species and the crystal after treatment. Single-crystal XRD analysis elucidated the structure of the crystal as the ate complex **4**·DME (Scheme 3),[8] which suggested that the NMR-visible species was a complex with the composition of **4**·18-C-6 (Scheme 3). Meanwhile, it was found that in DMSO without 18-C-6, the B$_2$pin$_2$/MeOK/**2** reaction system also produced the same complex **4** as the major species, since the recorded ^{1}H-NMR spectrum was identical to that of independently prepared **4**·DME recorded in DMSO (see the ESI for details†). The structure of **4** well accounted for the dearomatized pyridine ring revealed by NMR analysis.

With the pure ate complex **4**·DME in hand, we were able to assess its redox properties. Electrochemical study revealed that the THF solution of complex **4**·DME exhibited an irreversible oxidation wave at −1.11 V *versus* the Fc$^{+/0}$ couple, as determined by both cyclic voltammetry (CV) and differential pulse voltammetry (DPV) experiments (Fig. 2). The oxidation potential was similar to that of many reported SEDs,[3c–e] which allows for electron transfer to a variety of substrates.

The reaction between complex **4**·DME and 4-iodoanisole (**5**) also verified its electron donor character. By addition of **4** to excess iodoarene **5** in THF under room temperature, anisole (**6**) was produced in a good yield rather quickly (Scheme 4). The observation was in agreement with a mechanism involving SET-initiated carbon–iodine bond activation in iodoarene **5** to form an aryl radical, which then underwent a hydrogen atom transfer (HAT) from the solvent THF to form the reduction product **6**.
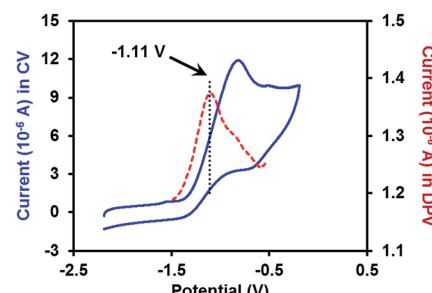

Fig. 2 CV and DPV plots of 2 mM complex **4**·DME in THF (0.1 M *n*-Bu$_4$N$^+$PF$_6^-$ as the supporting electrolyte). The blue solid line: CV plot (scan rate = 0.1 V s^{-1}); the red dashed line: DPV plot.

More interestingly, both *N,N'*-diboryl-2*H*,2'*H*-2,2'-bipyridine **7** and free pyridine **2** was observed by ^{1}H-NMR in the crude reaction mixture as the end-product of complex **4**, indicating that **4** served as an electron donor (*vide infra*). Notably, no trace of arylboronate was observed as the product in this reaction, even if the solvent was switched to DMSO to suppress the HAT pathway, indicating that complex **4** served merely as an electron donor, but not a borylation reagent.

Complex **4** represents an ate complex of pinacolato boronate with a *trans*-2*H*,2'*H*-[2,2'-bipyridine]-1,1'-diide unit as the ligand. This ate complex has not been reported previously, though several borate compounds with a 2,2'-bipyridine skeleton were reported. In 1992, Meller reported the formation of [1,3,2]-diazaborolobipyridine in the reaction between the pyridine radical anion and dialkylaminodifluorborane;[9] more recently, Tang and co-workers reported the reaction between isoquinoline and diboron to form a *N,N'*-diborate of 1,1',2,2'-tetrahydro-1,1'-bisisoquinoline.[10] However, these compounds were never found to exhibit any electron donor character. We attributed the electron-donating ability of complex **4** to both the dearomatized bipyridine scaffold and the negatively charged boron center. From a thermodynamic viewpoint, the cleavage of the B–B bond released the energy stored in the diboron and transferred it to the dearomatized bipyridine unit as the C–C bond formed. The negatively charged boron center may facilitate the loss of an electron from complex **4**, which induced the break of the bipyridine linkage and recovered the aromaticity of the pyridine ring. The dissociation of the bipyridine scaffold and the electron transfer of this complex were similar to the behavior of dihydropyridine dimers.[11]

Structure of EPR-visible species. The EPR spectrum of the B$_2$pin$_2$/MeOK/**2**/18-C-6 reaction mixture (Fig. 3a) indicated that some radical species were produced along with the boron–ate complex **4**. This spectrum was consistent with the previously
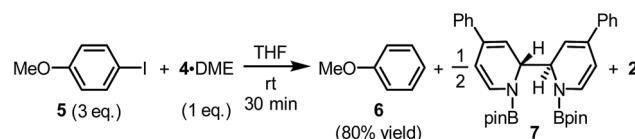
**Scheme 4** Electron donor character of complex **4**.
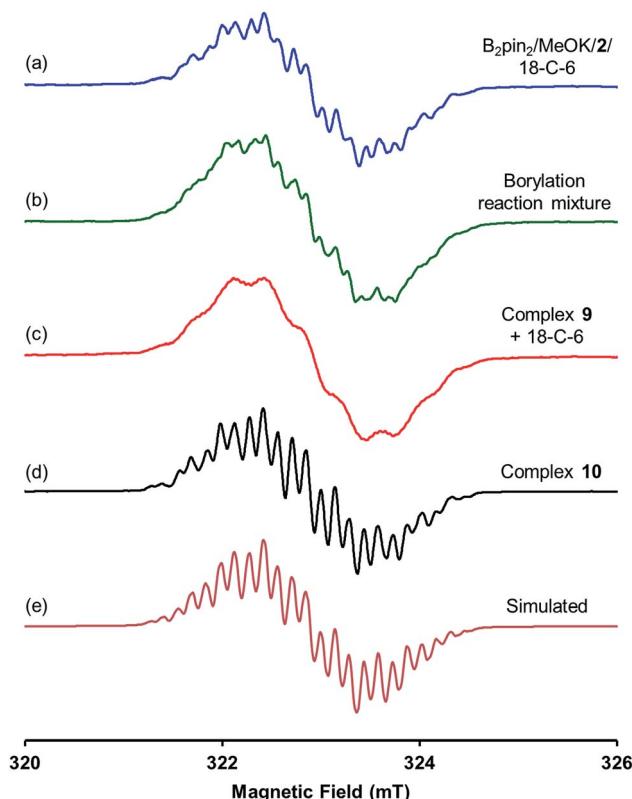
Fig. 3 X-band first derivative EPR spectra of (a) B_2pin_2/MeOK/2/18-C-6 reaction solution in THF; (b) the borylation reaction of 4-MeOPhBr employing B_2pin_2·MeOK/2 in DMSO; (c) the solution of complex 9 with 18-C-6 in THF; (d) the THF solution of complex 10 prepared by the reaction between 4-phenylpyridine radical anion and MeOBpin (all acquired at room temperature). (e) Is the simulated EPR spectrum with parameters listed in Table 1.

Scheme 5 Preparation of complexes 9 and 10. In the X-ray structure of 9, the sodium cation, the coordinating THF molecule, and hydrogen atoms are omitted for clarity. Thermal ellipsoids are drawn at 50% probability level.

recorded one of the borylation reaction mixture (Fig. 3b),[6] confirming that the same radical species also existed in the borylation reaction. However, the original proposal that both methoxyboronate radical anion (MeOBpin$^{•−}$) and pyridine-stabilized boryl radical (4-PhPy·Bpin$^•$) were generated in the reaction system was not reasonable due to the significantly unfavorable thermodynamics, as revealed by the DFT calculations (*vide infra*).

A hint for resolving the structure of the EPR-visible species came from a crystal structure obtained unexpectedly. When pyridine radical anion 8 (generated by treatment of pyridine 2 with sodium metal) was reacted with B_2pin_2 in THF, a deep purple crystal precipitated quickly instead of the light-yellow crystal of 4·DME obtained by the same reaction using DME as the solvent (Scheme 5). XRD analysis of the crystal revealed that it was a simple Lewis acid–base complex of the pyridine radical anion and the diboron derivative, denoted as 4-PhPy$^{•−}$·B_2pin_2 (9). Complex 9 could be re-dissolved in THF by the addition of 18-C-6, and EPR analysis of the solution showed a similar but significantly broadened spectrum compared to that of the reductive mixture (Fig. 3c). The formation of 9 indicated that the radical anion of pyridine could coordinate with a boron Lewis

acid center,[12] and the similar EPR spectrum also implied the structural relevance of the unknown radical species to complex 9.

We assumed that the EPR-visible species was also a complex of the 4-phenylpyridine radical anion and a boron Lewis acid. Methyl pinacolyl borate (MeOBpin) was the most probable one, because it existed as the byproduct in the B_2pin_2/MeOK/2 reaction system. To confirm this hypothesis, we conducted the reaction between pyridine radical anion 3 and MeOBpin (Scheme 5). It was found that upon addition of MeOBpin to a THF solution of 3, the color of the solution changed immediately from deep blue to deep purple, and it showed a well-resolved EPR spectrum, which exhibited similar spectral pattern and identical peak positions to the one obtained for the B_2pin_2/MeOK/2/18-C-6 mixture (Fig. 3d). Meanwhile, the addition of excess MeOBpin to a THF solution of complex 9 and 18-C-6 resulted in a similar EPR spectrum to that shown in Fig. 3a (Fig. S3 in the ESI†). These results suggested that the complex between the 4-phenylpyridine radical anion and MeOBpin, denoted as 4-PhPy$^{•−}$·B(OMe)pin (10), accounted for the EPR-visible radical species. Computer simulation of the recorded EPR spectrum[13] afforded the experimental hyperfine coupling constants (hfcs) of the proposed radical species (Fig. 3e), and the comparison with the DFT-calculated hfcs further supported the identity of this species (Table 1). The slightly broadened peak shape observed for the B_2pin_2/MeOK/2 mixture (Fig. 3a) could be attributed to the existence of both complexes 9 and 10 in the reaction system, as a combination of the EPR spectra of complexes 9 and 10 well reproduced the measured spectrum (Fig. S7 in the ESI†).

The comparison of the UV-vis spectrum of the reductive mixture and that of complex 9 also supported this structural assignment (Fig. 4a). In the UV-vis spectrum of the mixture containing complexes 4 and 10,[14] two absorptions were observed at 377 and 567 nm. These absorption bands were attributed to complex 10 due to the absence of corresponding absorptions for complex 4. The two absorption bands fitted well

Table 1 Experimental and computed hyperfine coupling constants for complex **10·THF**

hfcs/MHz	a (^{11}B)	a (N)	a (2H$_a$)	a (2H$_b$)	a (2H$_c$)	a (2H$_d$)	a (H$_e$)
Exptl.[a]	3.9	10.2	12.5	1.3	8.1	3.1	8.3
DFT[b]	−4.8	12.1	−10.4	1.2	−9.7	3.8	−12.5

[a] The hfcs obtained from simulation of the experimental EPR spectrum (g = 2.0030) using EasySpin software. Only the magnitudes, but not the signs of the hfcs could be derived. [b] DFT calculated hfcs at the UB3LYP/6-31+G(d) level for the model structure of **10·THF**.

with those of the radical anion complex **9** and were attributed to the same pyridine substructure. This observation confirmed the structural relevance of complexes **9** and **10** and the nature of complex **10** as a pyridine radical anion complex.

Similar to ate complex **4**, complex **10** was found to be a good electron donor. During the addition of iodoarene **5** to the mixture of complexes **4** and **10**, the bleaching of the two characteristic absorption bands (Fig. 4b) and the disappearance of the EPR signal were observed, which was indicative of the consumption of complex **10** by the iodoarene as an electron acceptor.

Overview of electron donors. Through the results presented above, we could conclude that the reaction between diboron, methoxide and 4-phenylpyridine proceeds smoothly to produce two boryl–pyridine complexes, ate complex **4** as the major species and radical anion complex **10** as the minor species (Scheme 6). Ate complex **4** could be detected by NMR, while the radical complex **10** was invisible in the NMR spectrum and could only be detected by EPR. The deep purple color of the reductive mixture came from radical anion complex **10** due to the absorption at 567 nm. Both of these diboron-derived complexes acted as super electron donors, which could reduce haloarenes through SET. These unprecedented findings not
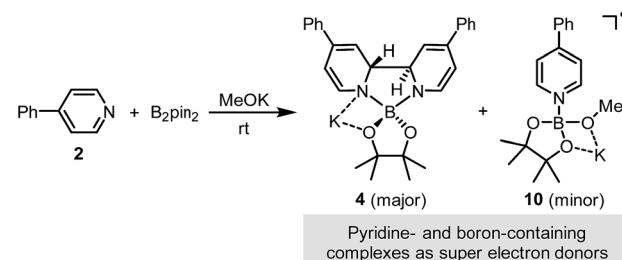
Scheme 6 Super electron donors in the reaction system.

only well rationalize the observed reactivity of the B$_2$pin$_2$/MeOK/pyridine system, but also demonstrate a novel way of preparing organic SEDs from easily accessible starting materials under mild conditions.

2. Mechanism for the formation of super electron donors

The key mechanistic problem for the formation of the two SED complexes in the reaction system was the mode of boron–boron bond cleavage. To solve this problem and to approach a clear mechanistic picture of this conversion, DFT computational study was conducted using the Gaussian 09 (ref. 15) software package. The geometric optimization was conducted at the M06-2X[16]/6-31+G(d) level of theory, and the frequency analysis was performed to verify the located structure to be either a minimum or a saddle point. Single-point energies were calculated at the M06-2X/6-311+G(d,p) level of theory, and the CPCM[17] method was used to evaluate the solvation effect in DMSO.

Homolytic cleavage pathway. Previous study by Li and Zhu established that diboron could undergo a homolytic cleavage in the presence of two molecules of 4-cyanopyridine to form two molecules of pyridine-stabilized boryl radical.[18] Given the observation that 4-phenylpyridine (**2**) could not cleave diboron without methoxide, the direct homolytic cleavage pathway was ruled out. Thus, we proposed a revised homolytic cleavage mechanism mimicking the established one by replacing one pyridine molecule with a methoxide anion in our previous work.[6]

This homolytic cleavage pathway was evaluated by DFT calculations in the present study (Fig. 5). The diboron first formed ate complex **IN1** with methoxide, which was already confirmed by the experimental studies of Marder *et al.*[19] Then pyridine **2** coordinated to the other vacant boron center in **IN1** to produce complex **IN2**, and this step is endergonic by 15.2 kcal mol^{-1} However, the proposed homolytic cleavage of the B–B bond in **IN2** was highly endergonic (by >30 kcal mol^{-1} from **IN1**), indicating that the formation of radical anion **IN3** and pyridine-stabilized boryl radical **IN4** from **IN2** was not feasible. Therefore, the mode of diboron cleavage promoted by 4-phenylpyridine and methoxide should be rather different from that promoted by 4-cyanopyridine.[18]

Heterolytic cleavage pathway. Alternatively, another mode of diboron cleavage was considered: the heterolytic cleavage of the B–B bond in complex **IN2** leading to MeOBpin and a boryl–
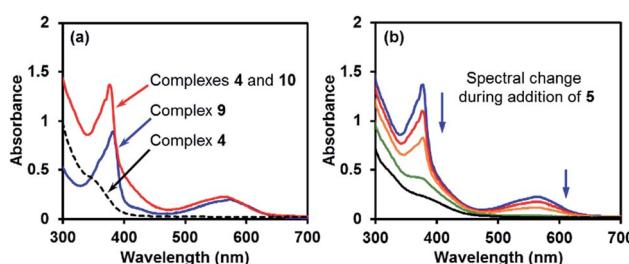
Fig. 4 (a) UV-vis spectra of the boryl–pyridine complexes in THF (red line: reaction mixture containing complexes **4** and **10**; blue line: solution of complex **9** and 18-C-6; dashed line: solution of complex **4·DME**). (b) UV-vis spectral change in the reaction mixture during the addition of iodoarene **5**.
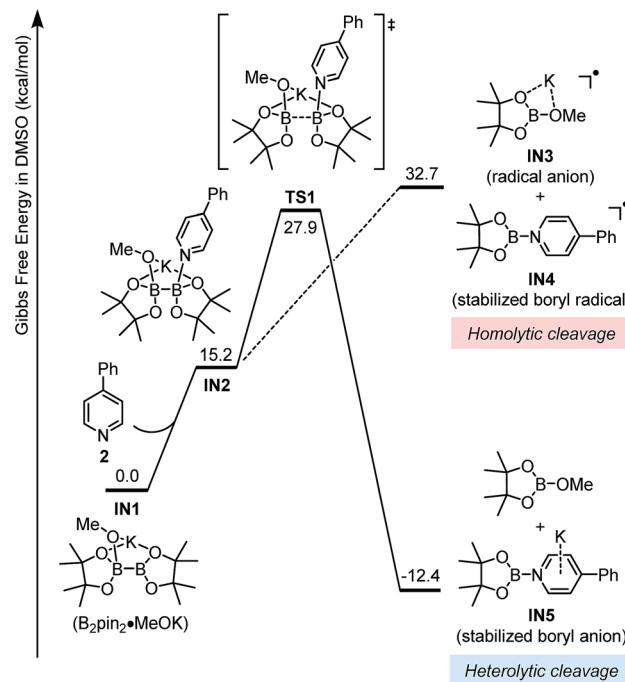
Fig. 5 Gibbs free energy ($\Delta G_{solv\ 298\ K}$) profile for the homolytic and heterolytic cleavage pathways of diboron.

pyridine anion complex **IN5** (Fig. 5). DFT calculation showed that this pathway is exergonic by 12.4 kcal mol^{-1} with an activation barrier of 27.9 kcal mol^{-1} in terms of Gibbs free energy. This renders the heterolytic cleavage pathway feasible both kinetically and thermodynamically. The cleavage step resembles the transfer of a boryl anion from the diboron to the pyridine moiety assisted by the methoxide anion. It is similar to the Lewis-base promoted heterolytic cleavage of diboron with simultaneous transfer of a boryl group to the acceptor *via* a nucleophilic attack,[20] though the pyridine derivative has never been found to be such an acceptor previously.

Intermediate **IN5** could be viewed as a complex between a boryl anion and a 4-phenylpyridine molecule or a so-called pyridine-stabilized boryl anion.[21] We proposed that **IN5** will be further transformed to complex **4**, and the potential energy surface for this transformation was calculated (Fig. 6). First, pyridine **2** in the reaction system could coordinate with the boron center of **IN5** through **TS2** to form a new complex **IN6**. Subsequently, intramolecular C–C bond formation occurs with a reasonable overall free energy barrier ($\Delta G^{\neq} = 23.1$ kcal mol^{-1} from **IN5**) to form the observed complex **4**. The overall conversion from **IN5** to complex **4** is exergonic by 2.1 kcal mol^{-1}.

[3,3]-Sigmatropic rearrangement pathway. Very recently, Tang and co-workers reported that isoquinoline reacts facilely with diboron *via* a [3,3]-sigmatropic rearrangement mechanism to form the *N,N′*-diborate of 1,1′,2,2′-tetrahydro-1,1′-bisisoquinoline.[10] This prompted us to consider an alternative mechanism for the formation of ate complex **4** (Scheme 7): the diboron reacts with pyridine **2** following a similar [3,3]-sigmatropic rearrangement mechanism to produce diboryl tetra-hydrobipyridine **7**, which then affords

complex **4** and MeOBpin in the presence of MeOK *via* a cyclization process.

In fact, it was found that heating a mixture of B$_2$pin$_2$ and pyridine **2** in DME resulted in the formation of **7**, together with some unidentified byproducts. Upon treatment with MeOK, **7** was smoothly transformed to complex **4**, as confirmed by ^{1}H-NMR analysis (Scheme 7). This indicated that compound **7** could act as a precursor to SED. However, the [3,3]-sigmatropic rearrangement pathway was not likely to operate in the present reaction system, because the reaction between B$_2$pin$_2$ and pyridine **2** proceeded rather sluggishly even at 100 °C, while the B$_2$pin$_2$/MeOK/**2**/18-C-6 reaction system showed >95% conversion within 2 h at room temperature. DFT calculation of the [3,3]-sigmatropic rearrangement mechanism also supported this conclusion, since a higher activation free energy barrier ($\Delta G^{\neq} = 30.0$ kcal mol^{-1}) rendered this pathway unfavorable compared with the heterolytic cleavage pathway ($\Delta G^{\neq} = 27.9$ kcal mol^{-1}).

Fig. 6 Gibbs free energy ($\Delta G_{solv\ 298\ K}$) profile for the formation of ate complex **4**.
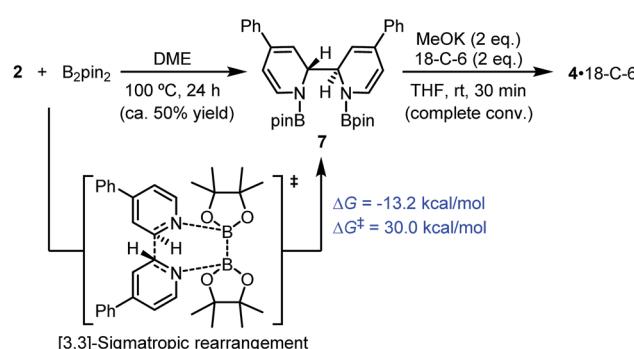

Scheme 7 [3,3]-Sigmatropic rearrangement pathway. DFT-calculated thermodynamic and kinetic parameters are shown in blue.

Formation of radical anion complex 10. It was observed that upon addition of MeOBpin to the independently synthesized complex 4·DME in THF, radical anion species **10** was produced immediately, as indicated by both UV-vis and EPR analysis (Scheme 8). ^{1}H-NMR analysis indicated incomplete conversion of **4** (*ca.* 20%), as well as the formation of compound **7** as the by-product. Because MeOBpin existed in the reaction system, it was reasonable to attribute the formation of complex **10** to the interaction between this Lewis acid and complex **4**.

A reasonable mechanism was proposed for this conversion with the aid of DFT calculation (Scheme 8). First, the Lewis acidic MeOBpin reacted with complex **4** to form a new complex, **IN7**, and this transformation was slightly endergonic. Then the homolytic cleavage of the bipyridine C2–C2′ bond led to both radical anion complex **10** and pyridine-stabilized boryl radical **IN4**, and this step was also slightly endergonic. Subsequently, radical species **IN4** dimerized to compound **7** rather facilely, as judged by the low activation free energy barrier and the thermodynamic driving force. The overall change in terms of Gibbs free energy was 0.1 kcal mol^{-1}, which was in agreement with the observed incomplete conversion.

In addition to this cleavage pathway, another pathway leading to complex **10** by direct SET was considered. Given that the anionic species **IN5** was highly electron rich, it may also act as an electron donor. We proposed that **IN5** could undergo SET with the complex of MeOBpin and pyridine **2** to produce complex **10** directly, and meanwhile **IN5** was transformed to radical **IN4** and then dimerized to **7**. This pathway was also feasible according to the DFT calculations (Scheme 9).

Interconversion of the boryl–pyridine intermediates. Based on the mechanism discussed above, a complete schematic presentation of the intermediates involved and their interconversion is shown in Fig. 7. Starting from stable compounds, a series of redox active boryl–pyridine intermediates were generated based on the formation of **IN5** *via* pyridine- and methoxide-promoted heterolytic cleavage of diboron. Among them, intermediates **IN5** and **IN4** were not directly observed due
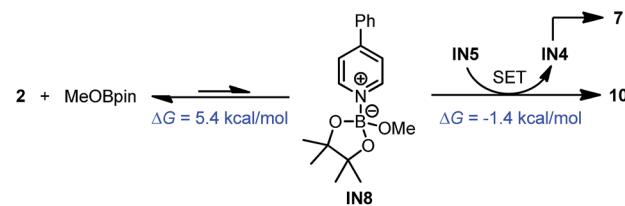
Scheme 9 Formation of complex **10** from **IN5**. DFT-calculated thermodynamic and kinetic parameters are shown in blue.

to their high activity, while compounds **4**, **10** and **7** were observed experimentally. The complexes **4** and **10** were the terminal products of this transformation network and constituted a major part of the reaction mixture. **IN5**, complex **4** and radical anion complex **10** are good electron donors due to their electron-rich nature; **IN4** and compound **7** are precursors to electron donors.

The SET pathways of the proposed SEDs are also summarized Fig. 7. After the electron transfer process, complex **IN5** produced pyridine-stabilized boryl radical **IN4**, which dimerized to afford compound **7**. Electron transfer from ate complex **4** resulted in the formation of both pyridine **2** and **IN4**, and then **IN4** produced dimer **7** rapidly. Radical anion complex **10** generated free pyridine **2** and MeOBpin upon losing an electron. Because compound **7** was proved a precursor to complex **4**, in the reaction system, **7** could be transformed to SED again with sufficient amount of methoxide. This transformation network realized an overall pyridine-catalyzed electron transfer process of B$_2$pin$_2$ + 2MeO$^-$ → 2MeOBpin + 2e$^-$, which rendered the diboron an efficient electron source.

3. Revised mechanism of the radical borylation reaction

The discovery of the real SED species in the diboron/methoxide/pyridine system prompted us to reconsider the mechanism of the radical borylation reaction based on this system. The generation of SEDs and the formation of aryl radical from the haloarene by SET have been made clear through the study presented above; however, the absence of boryl radical species **IN4** in the reaction mixture questioned the previously proposed cross-coupling mechanism between aryl radical and **IN4**.[6]

Figuring out the borylation reagent. Selective cross-coupling between the aryl radical and the pyridine-stabilized boryl radical **IN4** was proposed to rationalize the borylation process in our previous work, based on the assumption that **IN4** acts as a persistent radical.[6] However, the present study revealed that the dimerization of **IN4** to **7** was favorable both kinetically and thermodynamically (Scheme 8), and thus **IN4** could not accumulate to reach a reasonable concentration to enable efficient cross-coupling. Meanwhile, the reaction of iodoarene **5** with SED **4** did not produce any borylation product even during the formation of dimer **7** (Scheme 4), which unambiguously excluded both boryl radical **IN4** and its dimer **7** as the borylation reagent, as well as the SED complex **4**.

Interestingly, the reaction of iodoarene **5** with complex **4** in DMSO could produce the borylation product **11** only when
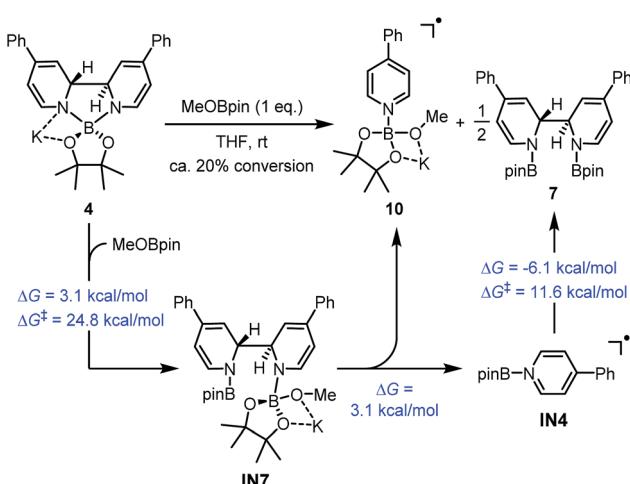
Scheme 8 Formation of complex **10** from complex **4**. DFT calculated thermodynamic and kinetic parameters are shown in blue.
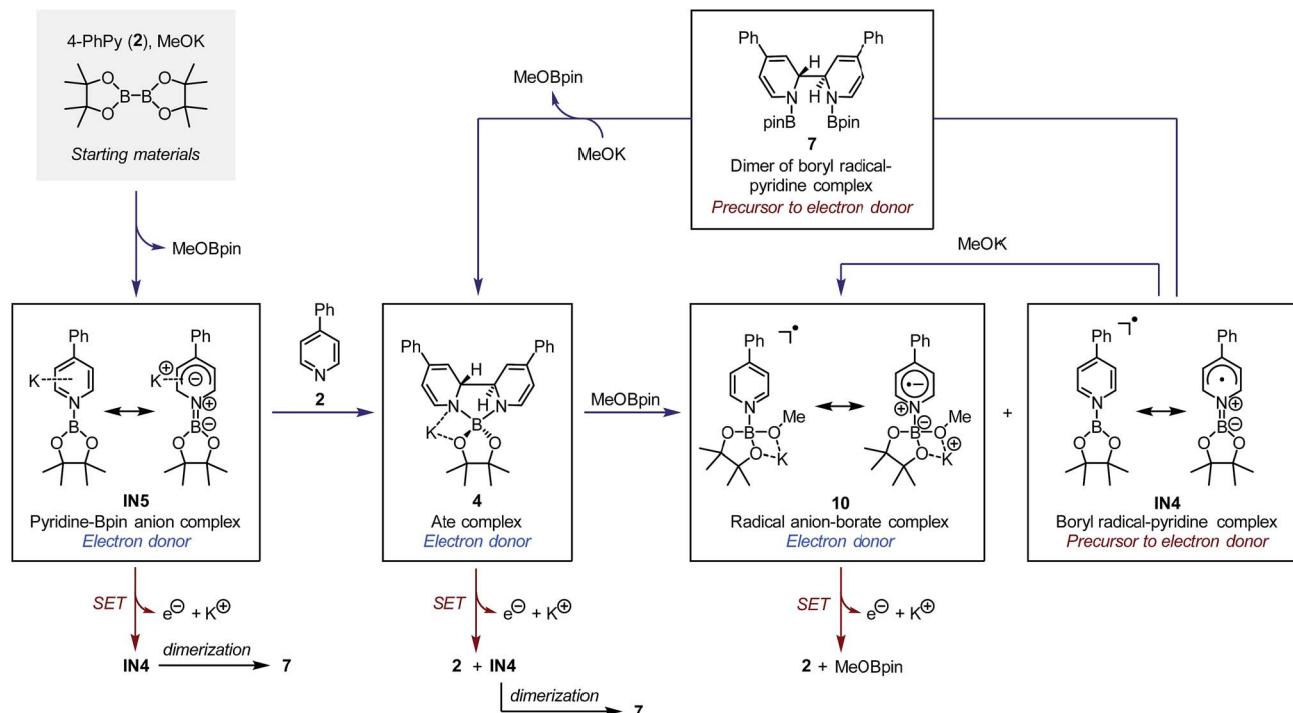
Fig. 7 Boryl–pyridine species involved in the reaction system and their interconversion. The blue arrows indicate the formation and interconversion between each species, while the red arrows indicate the single-electron transfer reaction of the electron donors.

B_2pin_2 was added. Crossover experiment using bis(hexylene glycolato)diboron in place of B_2pin_2 afforded the corresponding hexylene glycolyl boronate as the only borylation product (see the ESI for details†). These results indicated that diboron or its related species served as the borylation reagent. To figure out the very species that participates in the C–B bond formation event with the aryl radical, we conducted a series of competition experiments using the aryl radical cleanly generated from complex **4** and iodoarene **5** (Fig. 8). The experiments were conducted in a mixed solvent of THF and DMSO, and the ratio of arylboronate **11** (from borylation) to reduction product **6** (from HAT) was used as a measure of relative borylation rate. It was found that the concentration of pyridine **2** exhibited

a neglectable effect (Fig. 8a), while the concentration of B_2pin_2 had a perfect linear relationship with the ratio of **11** to **6** (Fig. 8b). In this kinetic competition scenario, the change in the relative borylation rate was affected merely by $[B_2pin_2]$, clearly indicating that the diboron itself rather than pyridine-containing boryl species (such as the complex between **2** and B_2pin_2 (ref. 22)) dictated the C–B bond formation step with the aryl radical.

Revisiting previous mechanistic conclusion. In our previous study, similar competition experiments were conducted employing iodoarene **5**, MeOK·B_2pin_2 ate complex and a variable amount of pyridine **2** in THF/DMSO mixed solvent.[6] The product distribution (the ratio of **11** to **6**) was found to be dependent on the concentration of **2**, which led to the conclusion that the radical borylation process occurred on a pyridine-related boryl species, with the radical species **IN4** being the most possible one.

That conclusion was distinct to the one drawn in the present study. By comparison of the reaction conditions used in both studies, we were able to figure out the reason for the difference. In the previous complex reaction system, MeOBpin was produced after the heterolytic cleavage of diboron by pyridine **2** and methoxide, and the effect of pyridine concentration on product distribution could be attributed to this Lewis acid: a higher concentration of pyridine **2** led to the production of more MeOBpin, which could release more B_2pin_2 from the MeOK·B_2pin_2 complex via ligand exchange equilibrium. The released diboron acted as the borylation reagent to favor the formation of the borylation product. In this way, the concentration of the free diboron was dictated by the concentration of
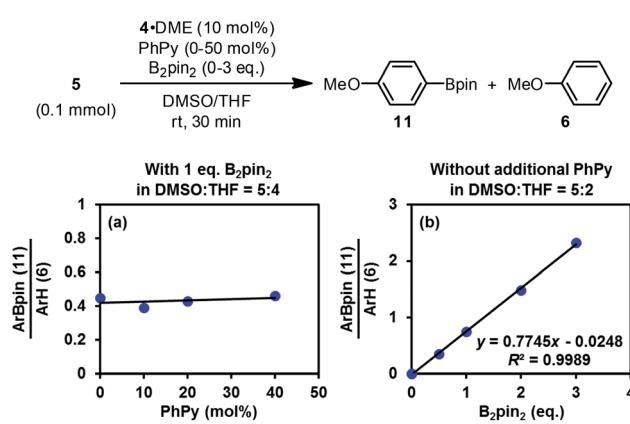
Fig. 8 Competition experiments.

pyridine **2**, which might be the reason for the apparent dependence of product distribution on pyridine **2**. In the present study, the clean and simple reaction system for aryl radical generation allowed for the investigation of the borylation process without interference of other factors, and thus we believed that the results obtained here are more reasonable.

With these new results in hand, currently, we propose a revised mechanism for the pyridine-catalyzed radical borylation (Scheme 10): the combination of diboron, MeOK and pyridine **2** produced SEDs **4** and **10**, which transformed a haloarene to an aryl radical by SET; the aryl radical reacted with the free diboron to produce arylboronate, which was proposed in several previous reports.[23] It was noteworthy that in the revised reaction mechanism, the borylation process was not subject to the persistent radical effect[24] but proceeded *via* a simple radical trapping mechanism. This feature would provide an opportunity for utilizing the present reaction system as an efficient tool for radical generation to access various functionalization products other than boronate, if the concentration of the free diboron could be controlled.

4. Application of the diboron-derived super electron donors in synthesis

The feature that super electron donors could be produced by simply mixing easily available and stable compounds would enable the application of the diboron/methoxide/pyridine system to various synthetically useful reactions, such as electron reduction reactions and electron-transfer-initiated radical chain reactions. In this study, we briefly explore its potential use in the synthesis as a proof of concept.

Reductive cleavage reactions. In addition to the C–X bond cleavage of haloarenes, the reductive cleavage of sulfonamide,[4c,25] *N*-oxy-substituted amide,[26] and *α*-oxy-substituted ketone[27] are classical organic redox reactions employing electron reductants. To test the synthetic utility of the present reaction system, we conducted the reductive cleavage reactions of substrates **12**, employing the mixture of B_2pin_2/MeOK/**2** as the source of the electron donor (Scheme 11). It was found that for *N*-tosylindole **12a**, Weinreb amides **12b–c** and *O*-acetylbenzoin **12d**, efficient single electron reduction and subsequent cleavage of the N–S, N–O and C–O bonds could be achieved. Control experiments revealed that these reduction reactions did not work in the absence of pyridine **2**. The replacement of the traditional electron reductants by a simple mixture rendered this method a practical alternative for electron reduction reactions.
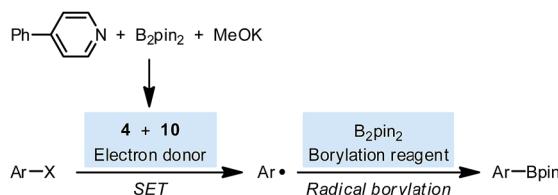

Scheme 10 Revised radical borylation mechanism.
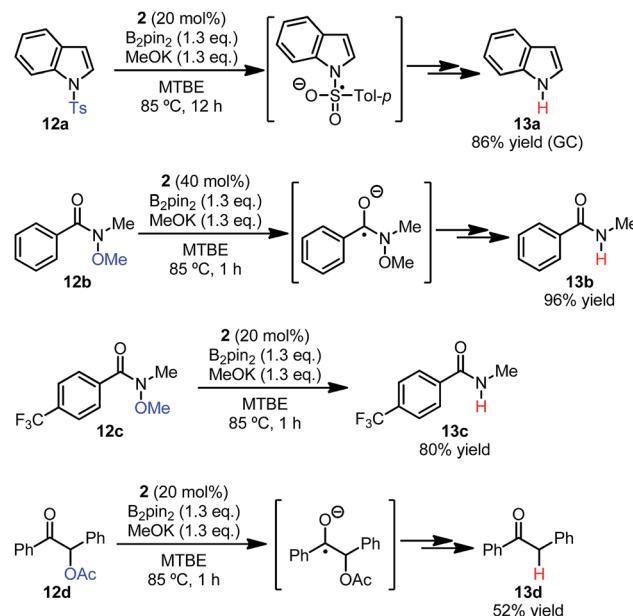
Scheme 11 Reductive cleavage reactions employing the diboron/MeOK/**2** system.

Initiation of radical chain reaction. Since efficient SET and radical generation could be promoted by the present reaction system, we believed that it had the potential to be used as a "radical initiator" to initiate radical chain reactions. Different from the reductive cleavage process, only a catalytic amount of the electron donor was required for initiating the radical chain reactions. To demonstrate this concept, the radical chain cyclization of **14** with n-Bu$_3$SnH was chosen as a model (Scheme 12),[28] where the *in situ* formed SEDs in the B_2pin_2/MeOK/**2** system (10 mol% each) was employed as the radical initiator in place of azobisisobutyronitrile (AIBN). Gratifyingly, under these conditions, the chain process proceeded smoothly to produce **15** in an excellent yield, and no borylation byproduct was formed. Without pyridine **2**, product
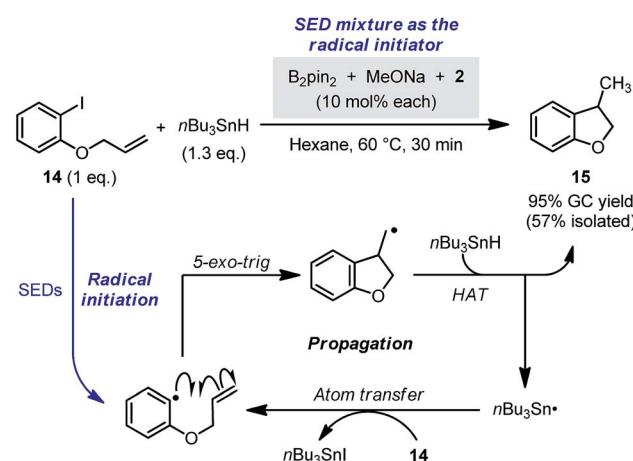
Scheme 12 Radical chain reaction initiated by the diboron-derived SEDs.

15 was only obtained in <10% yield. These results confirmed the ability of the diboron mixture to promote the SET-initiated radical chain reactions.

Compared with the radical initiation by thermolabile initiators, the present method allowed for fine-tuning of the initiation rate by controlling more factors (*e.g.*, concentration of each component, structure of each component, and temperature), which provides a more flexible option for the initiation of radical chain processes. Although with this single experiment we have merely showcased a simple proof of concept instead of extensively testing its usefulness, we think that the present method could contribute to the toolbox of radical chemistry.

Conclusions

In this work, a detailed study on the reaction system containing diboron, methoxide and 4-phenylpyridine was performed. This mixture was previously found to be effective for the borylation of haloarenes *via* a radical mechanism. With the discovery of two novel electron-donating boryl–pyridine species, the present study not only revealed the formation of super electron donors in the reaction system, but also showcased the value of this system as a practical single electron reducing agent.

Through a combined experimental and DFT computational study, we made clear the structures of two SEDs in the reaction system, as well as the mechanism for their formations. It was found that both the pyridine derivative and the methoxide anion were essential for the cleavage of the B–B bond in the diboron. In a complex of diboron with pyridine and methoxide coordinating to the two boron centers, heterolytic cleavage of the B–B bond, rather than previously assumed homolytic cleavage, occurred to form a methyl borate and a pyridine–boryl anion complex. In the presence of excess pyridine, these two intermediates were transformed to a *trans*-2H,2′H-[2,2′-bipyridine]-1,1′-diide borate complex and a pyridine radical anion–borate complex. These complexes were the major species observed in the reaction system, and their structures were determined by NMR, EPR and UV-vis spectroscopy and XRD analysis. Both complexes exhibited good electron-donating ability and were found to be novel SEDs not reported previously in literature. On the basis of these new findings, the mechanism of the pyridine-catalyzed radical borylation was revised.

The present reaction system represents the first example of utilizing diboron(4) compounds as the precursor to structurally well-defined single-electron reducing agents, and the SEDs derived from diboron have the potential to be used as a common single-electron reductant in organic synthesis. As our preliminary exploration revealed, in addition to the borylation reaction, this reaction system could be successfully applied to reductive cleavage reactions and radical chain cyclization reactions to replace common single-electron reductants. The features of these SEDs, such as the ease of preparation and the flexibility in structural tuning, make the present system a practical and promising complement to traditional electron donors. We seek to further investigate the structure–activity relationship of the reaction system, and expect that more applications in synthesis could be realized.

Conflicts of interest

There are no conflicts to declare.

Acknowledgements

Notes and references

1 (*a*) L. Eberson, *Electron Transfer Reactions in Organic Chemistry*, Springer-Verlag, Berlin, 1987; (*b*) *Encyclopedia of Radicals in Chemistry, Biology and Materials*, ed. C. Chatgilialoglu and A. Studer, Wiley, New York, 2012.

2 For selected examples and reviews, see: (*a*) N. D. Scott, J. F. Walker and V. L. Hansley, *J. Am. Chem. Soc.*, 1936, **58**, 2442; (*b*) P. Girard, J. L. Namy and H. B. Kagan, *J. Am. Chem. Soc.*, 1980, **102**, 2693; (*c*) W. A. Nugent and T. V. RajanBabu, *J. Am. Chem. Soc.*, 1988, **110**, 8561; (*d*) D. J. Procter, R. A. Flowers and T. Skrydstrup, *Organic Synthesis Using Samarium Diiodide: A Practical Guide*, RSC Publishing, Cambridge, 2010; (*e*) M. Szostak, N. J. Fazakerley, D. Parmar and D. J. Procter, *Chem. Rev.*, 2014, **114**, 5959; (*f*) A. Gansäuer and H. Bluhm, *Chem. Rev.*, 2000, **100**, 2771.

3 For earliest examples and reviews of electron donors, see: (*a*) C. Lampard, J. A. Murphy and N. Lewis, *J. Chem. Soc., Chem. Commun.*, 1993, 295; (*b*) N. Wiberg and J. W. Buchler, *Chem. Ber.*, 1963, **96**, 3223; (*c*) J. Broggi, T. Terme and P. Vanelle, *Angew. Chem., Int. Ed.*, 2014, **53**, 384; (*d*) J. A. Murphy, *J. Org. Chem.*, 2014, **79**, 3731; (*e*) E. Doni and J. A. Murphy, *Chem. Commun.*, 2014, **50**, 6073.

4 For selected examples of "super electron donors" as reagents, see: (*a*) J. A. Murphy, T. A. Khan, S. Z. Zhou, D. W. Thomson and M. Mahesh, *Angew. Chem., Int. Ed.*, 2005, **44**, 1356; (*b*) J. A. Murphy, S.-Z. Zhou, D. W. Thomson, F. Schoenebeck, M. Mohan, S. R. Park, T. Tuttle and L. E. A. Berlouis, *Angew. Chem., Int. Ed.*, 2007, **46**, 5178; (*c*) F. Schoenebeck, J. A. Murphy, S. Z. Zhou, Y. Uenoyama, Y. Miclo and T. Tuttle, *J. Am. Chem. Soc.*, 2007, **129**, 13368; (*d*) P. I. Jolly, S. Zhou, D. W. Thomson, J. Garnier, J. A. Parkinson, T. Tuttle and J. A. Murphy, *Chem. Sci.*, 2012, **3**, 1675; (*e*) J. A. Murphy, F. Schoenebeck, N. J. Findlay, D. W. Thomson, S. Z. Zhou and J. Garnier, *J. Am. Chem. Soc.*, 2009, **131**, 6475; (*f*) E. Cahard, F. Schoenebeck, J. Garnier, S. P. Y. Cutulic, S. Zhou and J. A. Murphy, *Angew. Chem., Int. Ed.*, 2012, **51**, 3673; (*g*) E. Doni, S. O'Sullivan and J. A. Murphy, *Angew. Chem., Int.*

Ed., 2013, **52**, 2239; (*h*) S. O'Sullivan, E. Doni, T. Tuttle and J. A. Murphy, *Angew. Chem., Int. Ed.*, 2014, **53**, 474; (*i*) E. Doni, B. Mondal, S. O'Sullivan, T. Tuttle and J. A. Murphy, *J. Am. Chem. Soc.*, 2013, **135**, 10934; (*j*) S. S. Hanson, E. Doni, K. T. Traboulsee, G. Coulthard, J. A. Murphy and C. A. Dyker, *Angew. Chem., Int. Ed.*, 2015, **54**, 11236.

5 For selected mechanistic study of "super electron donors" as reactive intermediates, see: (*a*) A. Studer and D. P. Curran, *Angew. Chem., Int. Ed.*, 2011, **50**, 5018; (*b*) A. Studer and D. P. Curran, *Nat. Chem.*, 2014, **6**, 765; (*c*) S. Zhou, G. M. Anderson, B. Mondal, E. Doni, V. Ironmonger, M. Kranz, T. Tuttle and J. A. Murphy, *Chem. Sci.*, 2014, **5**, 476; (*d*) S. Zhou, E. Doni, G. M. Anderson, R. G. Kane, S. W. MacDougall, V. M. Ironmonger, T. Tuttle and J. A. Murphy, *J. Am. Chem. Soc.*, 2014, **136**, 17818; (*e*) H. Yi, A. Jutand and A. Lei, *Chem. Commun.*, 2015, **51**, 545; (*f*) M. Patil, *J. Org. Chem.*, 2016, **81**, 632; (*g*) J. P. Barham, G. Coulthard, R. G. Kane, N. Delgado, M. P. John and J. A. Murphy, *Angew. Chem., Int. Ed.*, 2016, **55**, 4492; (*h*) L. Zhang, H. Yang and L. Jiao, *J. Am. Chem. Soc.*, 2016, **138**, 7151; (*i*) J. P. Barham, G. Coulthard, K. J. Emery, E. Doni, F. Cumine, G. Nocera, M. John, L. E. A. Berlouis, T. McGuire, T. Tuttle and J. Murphy, *J. Am. Chem. Soc.*, 2016, **138**, 7402; (*j*) M. Li, O. Gutierrez, S. Berritt, A. Pascual-Escudero, A. Yeşilçimen, X. Yang, J. Adrio, G. Huang, E. Nakamura-Ogiso, M. C. Kozlowski and P. J. Walsh, *Nat. Chem.*, 2017, **9**, 997; (*k*) M. Li, S. Berritt, L. Matuszewski, G. Deng, A. Pascual-Escudero, G. B. Panetti, M. Poznik, X. Yang, J. J. Chruma and P. J. Walsh, *J. Am. Chem. Soc.*, 2017, **139**, 16327; (*l*) H. Yang, L. Zhang and L. Jiao, *Chem.–Eur. J.*, 2017, **23**, 65.

6 L. Zhang and L. Jiao, *J. Am. Chem. Soc.*, 2017, **139**, 607.

7 For a review, see: (*a*) E. C. Neeve, S. J. Geier, I. A. Mkhalid, S. A. Westcott and T. B. Marder, *Chem. Rev.*, 2016, **116**, 9091; For examples employing diborons as reducing agents, see: (*b*) S. Bae and M. K. Lakshman, *J. Org. Chem.*, 2008, **73**, 1311; (*c*) H. P. Kokatla, P. F. Thomson, S. Bae, V. R. Doddi and M. K. Lakshman, *J. Org. Chem.*, 2011, **76**, 7842; (*d*) H. Lu, Z. Geng, J. Li, D. Zou, Y. Wu and Y. Wu, *Org. Lett.*, 2016, **18**, 2774; (*e*) K. Yang, F. Zhou, Z. Kuang, G. Gao, T. G. Driver and Q. Song, *Org. Lett.*, 2016, **18**, 4088; (*f*) M. Flinker, H. Yin, R. W. Juhl, E. Z. Eikeland, J. Overgaard, D. U. Nielsen and T. Skrydstrup, *Angew. Chem., Int. Ed.*, 2017, **56**, 15910.

8 Single crystals of **4**·DME were obtained by diffusion of solutions of B_2pin_2 (in hexane) and radical anion **3** (contained excess **2**, in DME) at 25 °C. Due to the labile nature of this complex, the obtained crystals are of insufficient qualities despite several attempts. Thus the quality of the acquired diffraction data was slightly below the average level (see the attached CIF file for details). Despite that, the present X-ray diffraction data confirmed the chemical structure of **4**·DME unambiguously.

9 W. Maringgele, A. Meller, S. Dielkus and R. Herbst-Irmer, *Z. Naturforsch., B: J. Chem. Sci.*, 1993, **48**, 561.

10 D. Chen, G. Xu, Q. Zhou, L. W. Chung and W. Tang, *J. Am. Chem. Soc.*, 2017, **139**, 9767.

11 For a review, see: (*a*) E. M. Kosower, *Top. Curr. Chem.*, 1983, **112**, 117; For examples, see: (*b*) E. M. Kosower and J. L. Cotter, *J. Am. Chem. Soc.*, 1964, **86**, 5524; (*c*) R. J. Gale and R. A. Osteryoung, *J. Electrochem. Soc.*, 1980, **127**, 2167; (*d*) F. Pragst and R. Stößer, *Z. Chem.*, 1985, **25**, 222; (*e*) F. Pragst and M. Šantrůček, *Adv. Synth. Catal.*, 1987, **329**, 67.

12 M. Grandl, B. Rudolf, Y. Sun, D. F. Bechtel, A. J. Pierik and F. Pammer, *Organometallics*, 2017, **36**, 2527.

13 The simulation of the experimental EPR spectra was performed using the EasySpin software package. See: S. Stoll and A. Schweiger, *J. Magn. Reson.*, 2006, **178**, 42.

14 A mixed solution of complexes **4** and **10**, prepared by the reaction between complex **4** and MeOBpin (see Scheme 8 and the ESI for details†), was used as the UV-vis sample in this study, because we were not able to isolate the pure form of complex **10**. Despite that, the existence of other species did not interfere with the assignment of the characteristic absorption bands of complex **10**.

15 For full citation of Gaussian 09, see the ESI.†

16 (*a*) Y. Zhao and D. G. Truhlar, *Theor. Chem. Acc.*, 2008, **120**, 215; (*b*) Y. Zhao and D. G. Truhlar, *Acc. Chem. Res.*, 2008, **41**, 157.

17 (*a*) V. Barone and M. Cossi, *J. Phys. Chem. A*, 1998, **102**, 1995; (*b*) M. Cossi, N. Rega, G. Scalmani and V. Barone, *J. Comput. Chem.*, 2003, **24**, 669.

18 (*a*) G. Wang, H. Zhang, J. Zhao, W. Li, J. Cao, C. Zhu and S. Li, *Angew. Chem., Int. Ed.*, 2016, **55**, 5985; (*b*) G. Wang, J. Cao, L. Gao, W. Chen, W. Huang, X. Cheng and S. Li, *J. Am. Chem. Soc.*, 2017, **139**, 3904.

19 (*a*) C. Kleeberg, L. Dang, Z. Li and T. B. Marder, *Angew. Chem., Int. Ed.*, 2009, **48**, 5350; (*b*) S. Pietsch, E. C. Neeve, D. C. Apperley, R. Bertermann, F. Mo, D. Qiu, M. S. Cheung, L. Dang, J. Wang, U. Radius, Z. Lin, C. Kleeberg and T. B. Marder, *Chem.–Eur. J.*, 2015, **21**, 7082.

20 For selected examples of the transition-metal-free heterolytic cleavage of boron–boron bond, see: (*a*) K. Lee, A. R. Zhugralin and A. H. Hoveyda, *J. Am. Chem. Soc.*, 2009, **131**, 7253; (*b*) A. Bonet, H. Gulyás and E. Fernández, *Angew. Chem., Int. Ed.*, 2010, **49**, 5130; (*c*) J. M. O'Brien and A. H. Hoveyda, *J. Am. Chem. Soc.*, 2011, **133**, 7712; (*d*) A. Bonet, C. Pubill-Ulldemolins, C. Bo, H. Gulyás and E. Fernández, *Angew. Chem., Int. Ed.*, 2011, **50**, 7158; (*e*) C. Solé, H. Gulyás and E. Fernández, *Chem. Commun.*, 2012, **48**, 3769; (*f*) K. Oshima, T. Ohmura and M. Suginome, *Chem. Commun.*, 2012, **48**, 8571; (*g*) C. Pubill-Ulldemolins, A. Bonet, C. Bo, H. Gulyás and E. Fernández, *Chem.–Eur. J.*, 2012, **18**, 1121; (*h*) H. Wu, S. Radomkit, J. M. O'Brien and A. H. Hoveyda, *J. Am. Chem. Soc.*, 2012, **134**, 8277; (*i*) T. P. Blaisdell, T. C. Caya, L. Zhang, A. Sanz-Marco and J. P. Morken, *J. Am. Chem. Soc.*, 2014, **136**, 9264; (*j*) L. Fang, L. Yan, F. Haeffner and J. P. Morken, *J. Am. Chem. Soc.*, 2016, **138**, 2508; (*k*) C. Kojima, K. H. Lee, Z. Lin and M. Yamashita, *J. Am. Chem. Soc.*, 2016, **138**, 6662; (*l*) Y. Katsuma, H. Asakawa, K.-H. Lee, Z. Lin and M. Yamashita, *Organometallics*, 2016,

35, 2563; (*m*) Y. Katsuma, H. Asakawa and M. Yamashita, *Chem. Sci.*, 2018, **9**, 1301.

21 For selected examples and reviews of six-electron boryl anions, see: (*a*) M. Yamashita and K. Nozaki, in *Synthesis and Application of Organoboron Compounds*, ed. E. Fernández and A. Whiting, Springer, Cham, 2015, vol. 49, pp. 1–37; (*b*) M. Yamashita and K. Nozaki, *Bull. Chem. Soc. Jpn.*, 2008, **81**, 1377; (*c*) Y. Segawa, M. Yamashita and K. Nozaki, *Science*, 2006, **314**, 113; For representative work about eight-electron boryl anions, see: (*d*) T. Imamoto and T. Hikosaka, *J. Org. Chem.*, 1994, **59**, 6753; (*e*) H. Braunschweig, C. W. Chiu, K. Radacki and T. Kupfer, *Angew. Chem., Int. Ed.*, 2010, **49**, 2041; (*f*) K. Nozaki, *Nature*, 2010, **464**, 1136; (*g*) R. Bertermann, H. Braunschweig, R. D. Dewhurst, C. Hörl, T. Kramer and I. Krummenacher, *Angew. Chem., Int. Ed.*, 2014, **53**, 5453.

22 A. Fawcett, J. Pradeilles, Y. Wang, T. Mutsuga, E. L. Myers and V. K. Aggarwal, *Science*, 2017, **357**, 283.

23 (*a*) A. M. Mfuh, J. D. Doyle, B. Chhetri, H. D. Arman and O. V. Larionov, *J. Am. Chem. Soc.*, 2016, **138**, 2985; (*b*) A. M. Mfuh, V. T. Nguyen, B. Chhetri, J. E. Burch, J. D. Doyle, V. N. Nesterov, H. D. Arman and O. V. Larionov, *J. Am. Chem. Soc.*, 2016, **138**, 8408; (*c*) W. Liu, X. Yang, Y. Gao and C. J. Li, *J. Am. Chem. Soc.*, 2017, **139**, 8621.

24 (*a*) H. Fischer, *Chem. Rev.*, 2001, **101**, 3581; (*b*) A. Studer, *Angew. Chem., Int. Ed.*, 2000, **39**, 1108; (*c*) A. Studer, *Chem. Soc. Rev.*, 2004, **33**, 267.

25 C. Najera and M. Jus, *Tetrahedron*, 1999, **55**, 10547.

26 G. E. Keck, T. T. Wager and S. F. McHardy, *Tetrahedron*, 1999, **55**, 11755.

27 A. Fuerstner, A. Hupperts, A. Ptock and E. Janssen, *J. Org. Chem.*, 1994, **59**, 5215.

28 A. L. J. Beckwith and W. B. Gara, *J. Chem. Soc., Perkin Trans. 2*, 1975, **7**, 795.